An Adaptive Energy Detection Technique Applied to Cognitive Radio Networks

Arash Vakili, Benoit Champagne
Department of Electrical and Computer Engineering
McGill University, Montreal, QC, Canada
arash.vakili@mail.mcgill.ca, benoit.champagne@mcgill.ca

***Abstract*—Spectrum sensing is an important functionality of cognitive radio as a means to detect the presence or absence of an existing user (EU), including the primary user or other secondary users, in a certain spectrum band. Energy detector (ED) is a widely used spectrum sensing technique based on the assumption that the EU is either present or absent during the whole sensing period. However, this assumption is not realistic in a dynamic environment where the EU could appear or disappear at any time. The performance of the conventional ED actually deteriorates in the scenario where the EU activity status changes during the sensing period. In this study, an adaptive ED is proposed to improve the detection performance in such dynamic environments. Analytical performance evaluation of the proposed adaptive ED along with simulation results prove its superiority over the conventional ED.**

I. Introduction

Measurement campaigns have shown that the available wireless spectrum is often not being used efficiently and cognitive radio (CR) technology has been proposed as a possible solution to the spectrum underutilization [1]. CR aims to sense the spectrum band licensed to the primary users (PUs), detect the unoccupied sub-bands, and opportunistically use them without interfering with the PUs or the other secondary users (SUs), jointly referred to as existing users (EUs). Spectrum sensing is indeed one of the main functionalities of CR as it allows to detect the unoccupied sub-bands (also called spectrum holes) and to avoid interference with the EUs.

Several spectrum sensing techniques have been proposed in the literature, including matched filtering [2], cyclostationary feature detection [3], and energy detection [4], [5]. If the SUs have adequate knowledge about the EU signal structure and/or modulation, matched filtering or cyclostationary feature detection can be used to maximize the probability of the EU signal detection at the expense of a more complex receiver. When such detailed *a-priori* knowledge of the EU signal is not available to the SUs, simple energy detector (ED) is generally preferred for spectrum sensing applications [6], [7].

The conventional ED is based on the assumption that the EU is either absent or present during the entire sensing period. This assumption could be valid for television broadcasting where a PU occupies or leaves the spectrum for a long time. However, it may not be realistic in a dynamic environment where the activity status of the EU could change at any time during the sensing period. It has been shown in [8] that the performance of the conventional ED deteriorates in scenarios where the EU appears during the sensing time, and an adaptive ED has been proposed to improve the detection. However, the equally important situation where an EU signal disappears during the sensing period is not considered.

In this paper, a novel adaptive ED is proposed which can address *both* of the aforementioned scenarios. The proposed technique is designed to improve the detection of a sudden change in the EU activity status by applying an adaptive exponential window over the received signal energies. In contrast with the former approach, where portion of the observations are discarded, our technique makes a better use of all the observations by properly weighting them. Analytical performance evaluation and simulation results prove that the proposed technique has superior performance over the conventional ED and also the adaptive ED in [8].

This paper is organized as follow. The system model and the limitations of the conventional ED performance are discussed in Section II. The proposed adaptive ED is developed under the two specified scenarios in Section III. Its performance analysis and numerical evaluation are presented in Section IV and Section V, respectively. This is followed by conclusion in Section VI. Regarding notations: $\mathcal{CN}(\mu, \sigma^2)$ refers to a circular symmetric complex Gaussian distribution with mean μ and variance σ^2, and $\chi^2(\nu)$ denotes a chi-square distribution with ν degrees of freedom. $Q(z)$ denotes the complementary distribution function of a standard normal random variable.

II. System model & Problem formulation

A. System model

Let $r(n)$ denote the complex baseband signal received by the SU after down-conversion and uniform sampling at the rate F_s. In the presence of an EU, this signal is represented as

$$r(n) = x(n) + w(n), \quad x(n) = \sum_{l=0}^{L-1} h(l)s(n-l), \quad (1)$$

where n denotes the sampling time index, $s(n)$ is the EU signal, $w(n)$ is the additive receiver noise, and $x(n)$ is the received EU signal at the output of the channel between the EU

This work is supported by InterDigital Canada Ltée., the Natural Sciences and Engineering Research Council of Canada, and the Government of Québec under the PROMPT program. A.Vakili also acknowledges a scholarship from Le Fonds Québécois de la Recherche sur la Nature et les Technologies.

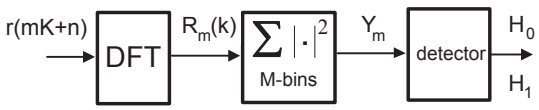

Fig. 1. Energy detection procedure (in practice, the DFT block is implemented by means of a fast Fourier transform (FFT))

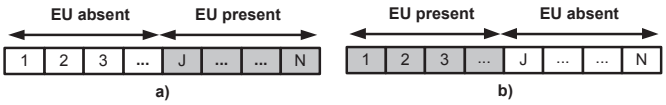

Fig. 2. Change of EU activity status during the sensing period: a) EU appearance b) EU disappearance

and the SU. This wireless channel is modeled as a linear time-invariant system with finite impulse response $h(n)$ of length L. It is assumed that the EU signal is unknown to the SU; therefore, the energy detector is optimum in this case [9].

In this paper, a frequency domain ED structure is considered as illustrated in Fig. 1. The received signal samples are divided into consecutive frames of K samples, and inputted to a K-point discrete Fourier transform (DFT) to obtain the narrow-band frequency components. The latter are represented analytically by:

$$R_m(k) = \frac{1}{\sqrt{K}} \sum_{n=0}^{K-1} r(mK+n) e^{-j2\pi nk/K}, \tag{2}$$

where $k = 0, ..., K-1$ is the frequency index (or frequency bin), $m = 1, ..., N$ is the frame index, and N is the total number of frames being processed by the SU. Similarly, let $X_m(k)$ and $W_m(k)$ denote the kth DFT coefficient of the mth frame of the channel output and the additive noise, i.e. $x(n)$ and $w(n)$ respectively. Then, it follows from (1) that

$$R_m(k) = X_m(k) + W_m(k). \tag{3}$$

In this work, $\{X_m(k)\}$ and $\{W_m(k)\}$ are modeled as two independent random processes. The samples of these two processes are independent across frequency and frame indices and follow a zero mean, circularly symmetric complex Gaussian distribution. Furthermore, it is assumed that the variances of the noise and the received signals, i.e. $E\{|W_m(k)|^2\} = \sigma_w^2$, and $E\{|X_m(k)|^2\} = \sigma_x^2$, are known from a priori estimation. For simplicity, we also let these quantities be independent of frequency, although generalizations are possible.

The energy of each frame is obtained by summing the squared magnitude of M frequency coefficients based on Parseval's theorem, which for the mth frame takes the form

$$Y_m = \sum_{k \in \mathcal{B}} |R_m(k)|^2, \tag{4}$$

where $\mathcal{B}$ is a set of M frequency bins corresponding to the bandwidth of interest. Finally, the frame energies Y_m are passed to a detection module where they are integrated and used to make a decision about the presence of an EU.

B. Problem Formulation

Conventional ED assumes that the EU activity status is constant during the entire sensing period of N frames, and a choice is made between two hypotheses $\mathcal{H}_0$ and $\mathcal{H}_1$, which represent the absence and presence of the EU signal, respectively:

$$\begin{aligned} \mathcal{H}_0 &: R_m(k) = W_m(k) \\ \mathcal{H}_1 &: R_m(k) = X_m(k) + W_m(k), \end{aligned} \tag{5}$$

where the given condition holds for all $m = 1, ..., N$ and $k \in \mathcal{B}$. Thus, under each hypothesis, the observed frequency samples $R_m(k)$ are independent and identically distributed, with $R_m(k) \sim \mathcal{CN}(0, \sigma_w^2)$ under $\mathcal{H}_0$ and $R_m(k) \sim \mathcal{CN}(0, \sigma_x^2 + \sigma_w^2)$ under $\mathcal{H}_1$.

For the above system model, the optimal binary detector computes a test statistic, T_N, by summing the measured energies of N frames, and comparing it against a threshold γ to choose between $\mathcal{H}_0$ and $\mathcal{H}_1$:

$$T_N = \sum_{m=1}^{N} Y_m \underset{\mathcal{H}_0}{\overset{\mathcal{H}_1}{\gtrless}} \gamma. \tag{6}$$

The performance of this detector can be easily analyzed in terms of its probabilities of detection and false alarm. In particular, Y_m (4) is the sum of squared magnitudes of complex Gaussian random variables and therefore, has a chi-square distribution under each hypothesis, with mean and variance given as follows:

$$\mu_{Y|0} = M\sigma_w^2, \quad \mu_{Y|1} = M(\sigma_w^2 + \sigma_x^2) \tag{7a}$$

$$\sigma_{Y|0}^2 = M\sigma_w^4, \quad \sigma_{Y|1}^2 = M(\sigma_w^2 + \sigma_x^2)^2, \tag{7b}$$

where $|0$ and $|1$ denote conditioning on the hypothesis where the EU signal is absent and present during a *single* frame, respectively. From there, the distribution of T_N and the performance of the detector (6) can be obtained.

Unfortunately, the above assumption that the EU activity status remains unchanged is not realistic in a dynamic environment where the EU could appear or disappear during the sensing period. Two scenarios of particular interest in this work are illustrated in Fig. 2 for the case that the SU allocates N frames for sensing. In both scenarios, the EU activity status is constant until it is changed on the Jth frame and it is assumed that the EU keeps that status for a period longer than sensing time. Part a) corresponds to the appearance of the EU, while part b) corresponds to its disappearance.

The performance of the classical detector (6) is now examined under the two aforementioned scenarios. Assuming that N or M are relatively large, the distribution of T_N can be approximated by central limit theorem as Gaussian under both scenarios, but with different first and second moments. In the appearing scenario, let $\mathcal{H}_0$ and $\mathcal{H}_1 \equiv \mathcal{H}_1(J)$ represent the absence of the EU signal (during the entire sensing period) and its appearance at the Jth frame, respectively. The mean

and variance of T_N under these two hypotheses are obtained as follows

$$\mu_{T|\mathcal{H}_0} = N\mu_{Y|0}$$
$$\mu_{T|\mathcal{H}_1} = (J-1)\mu_{Y|0} + (N-J+1)\mu_{Y|1} \quad (8a)$$
$$\sigma^2_{T|\mathcal{H}_0} = N\sigma^2_{Y|0}$$
$$\sigma^2_{T|\mathcal{H}_1} = (J-1)\sigma^2_{Y|0} + (N-J+1)\sigma^2_{Y|1}. \quad (8b)$$

The probability of the EU signal detection, P_d, is then obtained as

$$P_d = P(T_N > \gamma|\mathcal{H}_1) = Q(\frac{\gamma - \mu_{T|\mathcal{H}_1}}{\sigma_{T|\mathcal{H}_1}}), \quad (9)$$

where γ is the test threshold obtained for a given probability of false alarm, P_f, as

$$\gamma = Q^{-1}(P_f)\sigma_{T|\mathcal{H}_0} + \mu_{T|\mathcal{H}_0}, \quad (10)$$

where $P_f = P(T_N > \gamma|\mathcal{H}_0)$. The test statistic T_N under $\mathcal{H}_1$ is corrupted by the accumulation of noise power in the first $J-1$ frames, which causes the deterioration of P_d in this scenario. This fact has been confirmed by evaluating P_d in (9) under constant P_f for different values of J and a fixed N, as will be further discussed in Section V.

In the disappearing scenario, let $\mathcal{H}_1$ and $\mathcal{H}_0 \equiv \mathcal{H}_0(J)$ represent the presence of the EU signal (during the entire sensing period) and its disappearance at the Jth frame, respectively. The mean and variance of T_N under these two hypotheses are given as

$$\mu_{T|\mathcal{H}_0} = (J-1)\mu_{Y|1} + (N-J+1)\mu_{Y|0}$$
$$\mu_{T|\mathcal{H}_1} = N\mu_{Y|1} \quad (11a)$$
$$\sigma^2_{T|\mathcal{H}_0} = (J-1)\sigma^2_{Y|1} + (N-J+1)\sigma^2_{Y|0}$$
$$\sigma^2_{T|\mathcal{H}_1} = N\sigma^2_{Y|1}. \quad (11b)$$

In this case, the probability of spectrum hole detection, P_h, can be obtained as

$$P_h = P(T_N < \gamma|\mathcal{H}_0) = 1 - Q(\frac{\gamma - \mu_{T|\mathcal{H}_0}}{\sigma_{T|\mathcal{H}_0}}), \quad (12)$$

where γ is the test threshold corresponding to a desired P_d as follows:

$$\gamma = Q^{-1}(P_d)\sigma_{T|\mathcal{H}_1} + \mu_{T|\mathcal{H}_1}. \quad (13)$$

Here, the test statistic under $\mathcal{H}_0$ is corrupted by the accumulation of the EU signal energies in the first $J-1$ frames. Therefore, the probability of spectrum hole detection is degraded if $J > 1$. This can also be verified by evaluating P_h in (12) under constant P_d for different values of J and a fixed N (see Section V).

III. Proposed adaptive energy detector

The proposed adaptive ED procedure, shown in Fig. 3, borrows from conventional ED in that it measures the energy of the received signal samples in the frequency domain. However, as explained below, two adaptive mechanisms have been included to make this design more compatible to the dynamic environments mentioned in Section II-B.

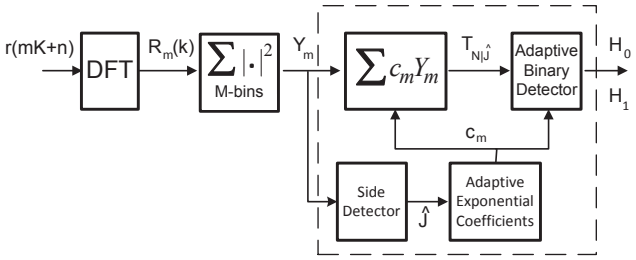

Fig. 3. Proposed adaptive ED procedure

In Fig. 3, the side detector compares individual frame energies Y_m to a pre-set threshold γ_s, to obtain a rough estimate of the true (but unknown) frame index J where the EU activity status changes. This estimate, $\hat{J}$, is applied to the input of an adaptive control mechanism which adjusts a set of exponential weighting coefficients, c_m for $m \in \{1, \ldots, N\}$, as follows:

$$c_m = \begin{cases} a^{(N-m)/(N-\hat{J})}, & \hat{J} < N \\ b^{N-m}, & \hat{J} = N \end{cases} \quad (14)$$

where a and b are user-defined parameters limited to the range $(0, 1)$. The collected frame energies are weighted by the exponential coefficients, and added together to obtain a conditional test statistic as follows

$$T_{N|\hat{J}} = \sum_{m=1}^{N} c_m Y_m. \quad (15)$$

The weighting coefficients c_m in (15) have the effect of reducing the accumulated energy in the first $J-1$ frames, which causes the deterioration of the detection probability in dynamic environments. These coefficients are in turns used by the adaptive binary detector mechanism to calculate the test threshold γ_a that maintains a desired performance, as given by P_f in the appearing scenario and P_d in the disappearing scenario. The conditional test statistics is then used to make the final decision via a binary test:

$$T_{N|\hat{J}} \underset{\mathcal{H}_0}{\overset{\mathcal{H}_1}{\gtrless}} \gamma_a. \quad (16)$$

Note that the above approach is different than the quickest detection approach in sequential change-point detection problems, where the goal is to minimize the detection delay subject to a certain false alarm constraint.

The functionality of the proposed adaptive ED is further detailed below for the two scenarios of interest.

A. Appearing scenario

In the appearing scenario, the side detector attempts to estimate the frame index, J, where the EU signal appears by applying ED on a frame-by-frame basis, using the threshold

$$\gamma_s = Q^{-1}(P_{fs})\sigma_{Y|0} + \mu_{Y|0}, \quad (17)$$

where $P_{fs} = P(Y_m > \gamma_s|0)$ is the desired probability of false alarm (for single frame processing) and $\mu_{Y|0}$ and $\sigma_{Y|0}$ are

defined in (7a)-(7b). The rough estimate $\hat{J}$ is obtained as the first value of m such that $Y_m > \gamma_s$; otherwise, if no such m can be observed, we set $\hat{J} = 1$. The estimate $\hat{J}$ is used to compute the exponential weights c_m as in (14).

As explained in Section II-B, Y_m has a chi-square distribution; hence the conditional test statistic in (15) is just a weighted sum of independent chi-squared random variables. Because the exact distribution of such a weighted sum is difficult to obtain in general, various approximations have been proposed [10]. One relatively simple and widely used approximation is to model this sum as a scaled chi-square random variable [11]. Specifically, based on this approximation, the distribution of $T_{N|\hat{J}}$ (15) is given by $\zeta_N \frac{\sigma_R^2}{2}\chi^2(2MN)$, where $\zeta_N = \frac{1}{N}\sum_{m=1}^{N} c_m$, and σ_R is the variance of $R_m(k)$ under the given hypothesis. The conditional mean and variance of $T_{N|\hat{J}}$ under $\mathcal{H}_0$ are then given by [1]

$$\mu_{T|\mathcal{H}_0} = \zeta_N N \mu_{Y|0} \tag{18a}$$
$$\sigma^2_{T|\mathcal{H}_0} = \zeta_N^2 N \sigma^2_{Y|0}. \tag{18b}$$

The adaptive detector block receives c_m and applies them into the above equations to update the test threshold, γ_a, to make the final decision. Assuming that N or M are relatively large, then $T_{N|\hat{J}}$ can be approximated as a Gaussian random variable [11]. Therefore, for a given P_f, the threshold γ_a is obtained as

$$\gamma_a = Q^{-1}(P_f)\sigma_{T|\mathcal{H}_0} + \mu_{T|\mathcal{H}_0}. \tag{19}$$

If $T_{N|\hat{J}}$ exceeds γ_a, then hypotheses $\mathcal{H}_1$ is selected; otherwise, $\mathcal{H}_0$ is declared as the current state of the channel.

The idea of deploying the side detector to estimate J for the appearing scenario, has already been used in [8]; However, in that work, the output of the side detector, $\hat{J}$, is used to eliminate the first $\hat{J}-1$ frames in order to improve the EU signal detection performance. In the proposed model, the side detector output, $\hat{J}$, is used instead to adjust the exponential weighting coefficients, c_m, in such a way that the accumulated energy in the first $\hat{J}-1$ frames are weighted less in comparison with the energy of the frames in the rest of the sensing period. This makes our proposed technique more robust to errors in the estimator $\hat{J}$, as it will be shown in section V.

B. Disappearing scenario

In the disappearing scenario, the threshold used by the side detector is

$$\gamma_s = Q^{-1}(P_{ds})\sigma_{Y|1} + \mu_{Y|1}, \tag{20}$$

where $P_{ds} = P(Y_m > \gamma_s|1)$ is the desired probability of EU signal detection for a single frame.The rough estimate $\hat{J}$ is obtained as the first value of m such that $Y_m < \gamma_s$; otherwise, we set $\hat{J} = 1$.

[1]The variance of $T_{N|\hat{J}}$ can be directly obtained using the fact that the random variables $Y_m, m = 1, ..., N$ are independent. The resulting variance $\sum_{m=1}^{N} c_m^2 \sigma^2_{Y|0}$ differs from the variance obtained by the approximation given in [11]. However, we have observed through simulations that the variance in (18b) results into better performance.

Similar to Section III-A, the mean and variance of $T_{N|\hat{J}}$ under $\mathcal{H}_1$ are given by

$$\mu_{T|\mathcal{H}_1} = \zeta_N N \mu_{Y|1} \tag{21a}$$
$$\sigma^2_{T|\mathcal{H}_1} = \zeta_N^2 N \sigma^2_{Y|1}. \tag{21b}$$

Using the above results, the adaptive binary detector adjusts the test threshold, γ_a, for a desired P_d as follows:

$$\gamma_a = Q^{-1}(P_d)\sigma_{T|\mathcal{H}_1} + \mu_{T|\mathcal{H}_1}, \tag{22}$$

and chooses between the two hypothesis using (16).

We finally note that the thresholds of the two adaptive mechanisms are different depending on the scenario of interest. A SU should employ the appearing scenario's thresholds for the case that it is already transmitting data and it is sensing the spectrum for the PU appearance. On the other hand, a SU should use the disappearing scenario's thresholds for the case that it is sensing for an unoccupied spectrum band.

IV. Performance Analysis

The analytical performance of the proposed adaptive ED is investigated under the two scenarios of interest. This means that the parameter J is considered to be known and the probability of detection is calculated analytically for each scenario.

A. Appearing scenario

As it was explained in Section III-A, the operation of the adaptive binary detector is based on the calculated weighting coefficients c_m. These coefficients are dependent on $\hat{J}$; therefore, using the statistics of $T_{N|\hat{J}}$, the probability of the EU signal detection *conditioned* on $\hat{J}$ is obtained as follows:

$$P_{d|\hat{J}} = P(T_{N|\hat{J}} > \gamma_a|\mathcal{H}_1) = Q(\frac{\gamma_a - \mu_{T|\mathcal{H}_1}}{\sigma_{T|\mathcal{H}_1}}), \tag{23}$$

where γ_a is the threshold of the adaptive binary detector block in (19). Here $\mu_{T|\mathcal{H}_1}$ and $\sigma^2_{T|\mathcal{H}_1}$ represent the mean and the variance of $T_{N|\hat{J}}$ under $\mathcal{H}_1$ and are given by

$$\mu_{T|\mathcal{H}_1} = \zeta_A A \mu_{Y|0} + \zeta_B B \mu_{Y|1} \tag{24a}$$
$$\sigma^2_{T|\mathcal{H}_1} = \zeta_A^2 A \sigma^2_{Y|0} + \zeta_B^2 B \sigma^2_{Y|0}, \tag{24b}$$

where $A = J - 1$, $B = N - J + 1$, $\zeta_A = \frac{1}{A}\sum_{m=1}^{J-1} c_m$, and $\zeta_B = \frac{1}{B}\sum_{m=J}^{N} c_m$.

Finally, the probability of EU signal detection is obtained by averaging (23) as

$$P_d = \sum_{\hat{J}=1}^{N} P_{d|\hat{J}}\, p(\hat{J}|\mathcal{H}_1), \tag{25}$$

where $p(\hat{J}|\mathcal{H}_1)$ is the probability mass function (PMF) of $\hat{J}$ under $\mathcal{H}_1$, obtained as follows. The side detector applies energy detection on every frame until the first frame energy that exceeds γ_s; therefore, this process is modelled as a Bernoulli

distribution with probabilities of "success" ($Y_m > \gamma_s$) under the two frame-hypotheses as

$$p_0 = P(Y_m > \gamma_s|0) = Q(\frac{\gamma_s - \mu_{Y|0}}{\sigma_{Y|0}}) \quad (26)$$

$$p_1 = P(Y_m > \gamma_s|1) = Q(\frac{\gamma_s - \mu_{Y|1}}{\sigma_{Y|1}}). \quad (27)$$

Here, γ_s is the side detector's threshold given in (17). Consequently, the probability of the "failure" ($Y_m < \gamma_s$) under frame-hypothesis 0 and 1 are defined as $q_0 = 1 - p_0$ and $q_1 = 1 - p_1$, respectively. Therefore, $\hat{J}$ has a "generalized" geometric distribution with PMF under $\mathcal{H}_1$ given as

$$p(\hat{J}|\mathcal{H}_1) = \begin{cases} p_0 + q_0^{J-1} q_1^{N-J+1} & \hat{J} = 1 \\ q_0^{\hat{J}-1} p_0 & 1 < \hat{J} < J \\ q_0^{J-1} q_1^{\hat{J}-J} p_1 & J \le \hat{J} \le N. \end{cases} \quad (28)$$

The performance of the proposed adaptive ED under the appearing scenario can be evaluated analytically based on (25). The evaluation results will be presented in section V.

B. Disappearing scenario

The same procedure as in Section IV-A is followed here with the exception that now the probability of hole detection, P_h, is under consideration, which is given by

$$P_h = \sum_{\hat{J}=1}^{N} P_{h|\hat{J}} p(\hat{J}|\mathcal{H}_0). \quad (29)$$

The conditional probability of hole detection, $P_{h|\hat{J}}$, is obtained as follows:

$$P_{h|\hat{J}} = P(T_{N|\hat{J}} < \gamma_a|\mathcal{H}_0) = 1 - Q(\frac{\gamma_a - \mu_{T|\mathcal{H}_0}}{\sigma_{T|\mathcal{H}_0}}), \quad (30)$$

where γ_a is given in (22). $\mu_{T|\mathcal{H}_0}$ and $\sigma_{T|\mathcal{H}_0}$ are the mean and the variance of $T_{N|\hat{J}}$ under $\mathcal{H}_0$, which are given by

$$\mu_{T|\mathcal{H}_0} = \zeta_A A \mu_{Y|1} + \zeta_B B \mu_{Y|0} \quad (31a)$$

$$\sigma^2_{T|\mathcal{H}_0} = \zeta^2_A A \sigma^2_{Y|1} + \zeta^2_B B \sigma^2_{Y|0}, \quad (31b)$$

where A, B, ζ_A, and ζ_B are defined in Section IV-A. The PMF of $\hat{J}$ under $\mathcal{H}_0$, $p(\hat{J}|\mathcal{H}_0)$, is obtained using a similar procedure as in the appearing scenario. The probability that the side detector declares the EU signal disappearance is given under the two frame-hypotheses as follows:

$$p_0 = P(Y_m < \gamma_s|0) = 1 - Q(\frac{\gamma_s - \mu_{Y|0}}{\sigma_{Y|0}}) \quad (32)$$

$$p_1 = P(Y_m < \gamma_s|1) = 1 - Q(\frac{\gamma_s - \mu_{Y|1}}{\sigma_{Y|1}}), \quad (33)$$

where γ_s is the threshold of the side detector in (20). Therefore, the PMF of $\hat{J}$ under $\mathcal{H}_0$ is obtained as

$$p(\hat{J}|\mathcal{H}_0) = \begin{cases} p_1 + q_1^{J-1} q_0^{N-J+1} & \hat{J} = 1 \\ q_1^{\hat{J}-1} p_1 & 1 < \hat{J} < J \\ q_1^{J-1} q_0^{\hat{J}-J} p_0 & J \le \hat{J} \le N. \end{cases} \quad (34)$$

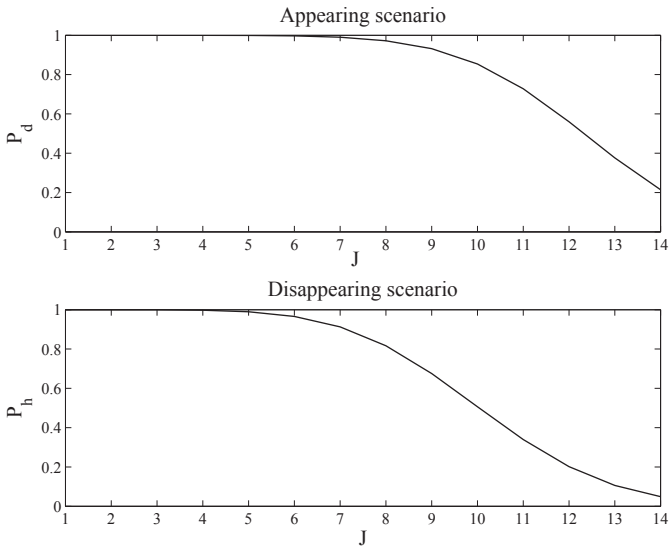

Fig. 4. Performance degradation of the conventional ED under appearing and disappearing scenario for $N = 14$

Finally, (29) is used to evaluate the performance of the proposed adaptive ED analytically under the disappearing scenario.

V. Simulation Results

In this section, the performance of the proposed adaptive ED and the conventional ED are investigated for dynamic scenarios where the EU activity status changes during the sensing period. An EU signal with a bandwidth of 200kHz is assumed to be sampled at a frequency of 1600kHz, and a 1024-point FFT is used to obtain the frequency representation of the signal. The bandwidth of interest corresponds to 128 frequency bins, i.e., $M = 128$. The received signal SNR is equal to -8dB, with desired $P_f = P_{fs} = 0.1$ and $P_d = P_{ds} = 0.98$ in the appearing and disappearing scenarios, respectively. The parameters in (14) are set to $a = 0.2$ and $b = 0.5$, based on preliminary experiments.

The performance deterioration of the conventional ED in dynamic scenarios is first investigated based on the analytical expressions (9) and (12) obtained in Section II. To this end, the number of sensing frames is set to $N = 14$ and the value of J (the frame index where the EU activity status changes) is varied from 1 to 14. The results are shown in Fig. 4 where it is observed that the probability of detection deteriorates significantly as J increases, specially for $J > N/2$.

In the rest of the simulations, J is set to 9 and N is varied from 9 to 14. For both the conventional ED and the proposed adaptive ED, random data are generated based on the model introduced in Section II-A and the simulations are run for 1000 independent trials to obtain an estimation of P_d and P_h for the appearing and disappearing scenarios, respectively. The results of these experiments are illustrated with the solid lines for the two scenarios in Fig. 5 and 6. These figures also include the theoretical results (dashed lines) which are

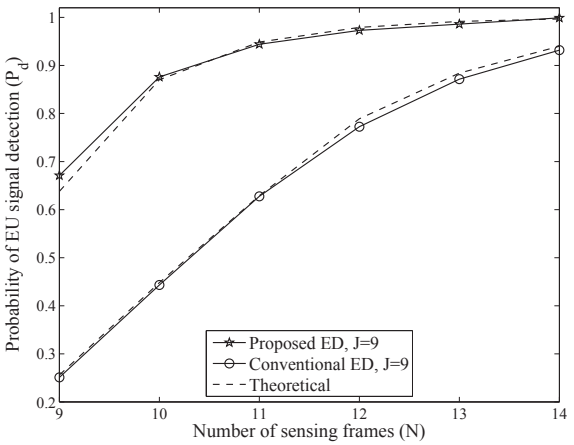

Fig. 5. Probability of the EU signal detection of the proposed adaptive ED compared with the conventional ED in the appearing scenario

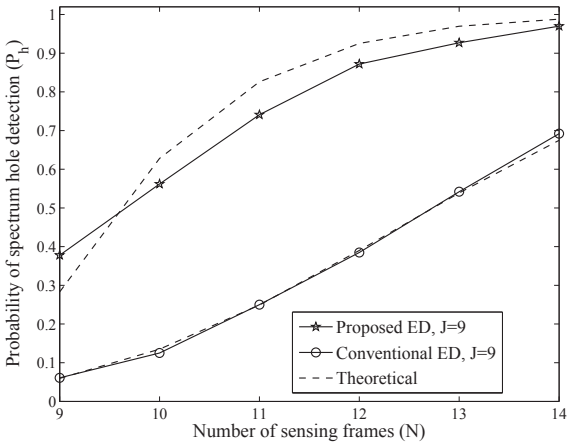

Fig. 6. Probability of the spectrum hole detection of the proposed adaptive ED compared with the conventional ED in the disappearing scenario

based on the analytical formulae obtained in Sections II and IV. It is observed that the proposed adaptive ED achieves a better performance compared to the conventional ED in both scenarios. Furthermore, the experimental results closely follow the analytical results.

As explained in Section III-A, the adaptive ED in [8] is intended to improve the probability of detection in the appearing scenario; therefore, it is reasonable to compare its performance to that of the adaptive ED proposed in this paper. These two adaptive EDs achieve a better performance, compared to the conventional ED, in exchange of an increase in P_f. Hence, the test thresholds obtained by both adaptive detectors need to be adjusted through simulations in order to maintain a desired P_f and thus a fair comparison. The result of such comparison is shown in Fig. 7 and it is observed that the proposed adaptive ED outperforms the alternative approach.

VI. Conclusion

The performance of the conventional ED is degraded in a dynamic environment where the EU activity status changes

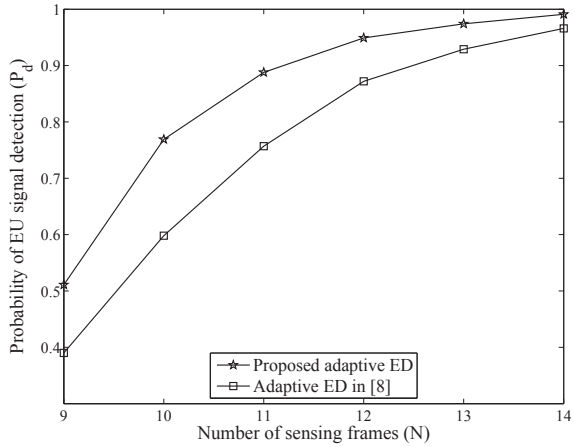

Fig. 7. Performance comparison of the proposed adaptive ED and the adaptive ED in [8] for the appearing scenario ($J = 9$)

during sensing period. An adaptive ED was proposed to improve the probability of detection in such environments. The proposed technique applies an exponential weighting window over the measured energies of N frames and adjusts the weighting coefficients based on estimated location of the frame where the EU activity status changes. Analytical performance analysis and simulations have proven the superiority of this technique over the conventional ED and the adaptive ED in [8].

References

[1] A. Ghasemi and E. S. Sousa, "Spectrum sensing in cognitive radio networks: requirements, challenges and design trade-offs," *IEEE Commun. Magazine*, vol. 46, no. 4, pp. 32–39, Apr. 2008.

[2] D. Cabric, A. Tkachenko, and R. Brodersen, "Spectrum sensing measurements of pilot, energy, and collaborative detection," in *IEEE Military Commun. Conf.*, pp. 1–7, Oct. 2006.

[3] K.-L. Du and W. H. Mow, "Affordable cyclostationarity-based spectrum sensing for cognitive radio with smart antennas," *IEEE Transactions on Vehicular Technology*, vol. 59, no. 4, pp. 1877–1886, May. 2010.

[4] K. Kim, Y. Xin, and S. Rangarajan, "Energy detection based spectrum sensing for cognitive radio: An experimental study," in *IEEE Global Telecommun. Conf.*, pp. 1–5, Dec. 2010.

[5] F. F. Digham, M.-S. Alouini, and M. K. Simon, "On the energy detection of unknown signals over fading channels," *IEEE Trans. on Commun.*, vol. 55, no. 1, pp. 21–24, Jan. 2007.

[6] Q. Zhi, C. Shuguang, A. H. Sayed, and H. V. Poor, "Optimal multiband joint detection for spectrum sensing in cognitive radio networks," *IEEE Trans. on Signal Processing*, vol. 57, no. 3, pp. 1128–1140, Mar. 2009.

[7] K. Hossain and B. Champagne, "Wideband spectrum sensing for cognitive radios with correlated subband occupancy," *IEEE Signal Processing Letters*, vol. 18, no. 1, pp. 35–38, Jan. 2011.

[8] T. S. Shehata and M. El-Tanany, "A novel adaptive structure of the energy detector applied to cognitive radio networks," in *11th Canadian Workshop on Information Theory*, pp. 95–98, Jun. 2009.

[9] S. M. Kay, *Fundamentals of Statistical Signal Processing: Detection Theory,*, vol. 2. Prentice Hall, NJ, USA, 1998.

[10] H. Solomon and M. A. Stephens, "Distribution of a sum of weighted chi-square variables," *Journal of the American Statistical Association*, vol. 72, no. 360, pp. 881–885, Dec. 1977.

[11] K.-H. Yuan and P. Bentler, "Two simple approximation to the distribution of quadratic forms," *British Journal of Mathematical and Statistical Psychology*, vol. 63, no. 2, pp. 273–291, May. 2010.